SIAM J. SCI. COMPUT.
Vol. 26, No. 2, pp. 558–577

A COMPARATIVE STUDY ON UNCERTAINTY QUANTIFICATION FOR FLOW IN RANDOMLY HETEROGENEOUS MEDIA USING MONTE CARLO SIMULATIONS AND CONVENTIONAL AND KL-BASED MOMENT-EQUATION APPROACHES*

ZHIMING LU† AND DONGXIAO ZHANG†‡

Abstract. Geological formations are ubiquitously heterogeneous, and the equations that govern flow and transport in such formations can be treated as stochastic partial differential equations. The Monte Carlo method is a straightforward approach for simulating flow in heterogeneous porous media; an alternative based on the moment-equation approach has been developed in the last two decades to reduce the high computational expense required by the Monte Carlo method. However, the computational cost of the moment-equation approach is still high. For example, to solve head covariance up to first order in terms of σ_Y^2, the variance of log hydraulic conductivity $Y = \ln K_s$, it is required to solve sets of linear algebraic equations with N unknowns for $2N$ times (N being the number of grid nodes). The cost is even higher if higher-order approximations are needed. Zhang and Lu [*J. Comput. Phys.*, 194 (2004), pp. 773–794] developed a new approach to evaluate high-order moments (fourth order for mean head in terms of σ_Y, and third order for head variances in terms of σ_Y^2) of flow quantities based on the combination of Karhunen–Loève decomposition and perturbation methods. In this study, we systematically investigate the computational efficiency and solution accuracy of three approaches: Monte Carlo simulations, the conventional moment-equation (CME) approach, and the moment-equation approach based on Karhunen–Loève decomposition (KLME). It is evident that the computational cost for the KLME approach is significantly lower than those required by the Monte Carlo and CME approaches. More importantly, while the computational costs (in terms of the number of times for solving linear algebraic equations with N unknowns) for the CME approach depend on the number of grid nodes, the cost for the KLME approach is independent of the number of grid nodes. This makes it possible to apply the KLME method to solve more realistic large-scale flow problems.

Key words. Monte Carlo simulations, moment-equation approach, Karhunen–Loève decomposition, heterogeneity, flow and transport, porous media

AMS subject classifications. 65C05, 65C30, 49N27, 76S05, 78M05, 82C31

DOI. 10.1137/S1064827503426826

1. Introduction.

Owing to heterogeneity of geological formations and incomplete knowledge of medium properties, the medium properties are treated as random space functions and the equations describing flow and transport in these formations become stochastic. Stochastic approaches to flow and transport in heterogeneous porous media have been extensively studied in the past two decades, and many stochastic models have been developed [7, 9, 4, 35].

Monte Carlo simulation is a conceptually straightforward method for solving these stochastic partial differential equations. It entails generating a large number of equally likely random realizations of the parameter fields, solving deterministic flow and trans-

*Received by the editors April 30, 2003; accepted for publication (in revised form) September 30, 2003; published electronically December 22, 2004. This work was supported by DOE/NGOTP under contract AC1005000. This work was performed by an employee of the U.S. Government or under U.S. Government contract. The U.S. Government retains a nonexclusive, royalty-free license to publish or reproduce the published form of this contribution, or allow others to do so, for U.S. Government purposes. Copyright is owned by SIAM to the extent not limited by these rights.

http://www.siam.org/journals/sisc/26-2/42682.html

†Hydrology, Geochemistry, and Geology Group (EES-6), MS T003, Los Alamos National Laboratory, Los Alamos, NM 87545 (zhiming@lanl.gov, donzhang@lanl.gov).

‡Current address: Mewbourne School of Petroleum and Geological Engineering, University of Oklahoma, 100 East Boyd, SEC T301, Norman, OK 73019.

port equations for each realization, and averaging the results over all realizations to obtain sample statistical moments of the solution. This approach has the advantage of applying to a broad range of both linear and nonlinear flow and transport problems. However, it also has a number of potential drawbacks [30, 17]. A major disadvantage of the Monte Carlo method, among others, is the requirement for large computational efforts. To properly resolve high-frequency space-time fluctuations in random parameters, it is necessary to employ fine numerical grids in space-time. Therefore, computational efforts for each realization are usually large. To ensure the convergence of the sample moments to their theoretical ensemble values, a large number of realizations are often required (typically a few thousand realizations, depending on the degree of medium heterogeneity), which poses a significant computational burden.

An alternative to Monte Carlo simulations is an approach based on moment equations, the essence of which is to derive a system of deterministic partial differential equations governing the statistical moments of the flow and transport quantities (usually the first two moments, mean and covariance) and then solve them analytically or numerically [5, 6, 7, 10, 32, 33, 16, 26, 28, 25, 38, 8, 21, 20, 19, 34, 35, 17].

The moment equations are usually derived with the method of perturbation. In the perturbation-based approach, the medium properties, such as log hydraulic conductivity Y, can be written as $Y = \langle Y \rangle + Y'$, and similarly the predicted quantity, such as hydraulic head h, can be decomposed as $h = \langle h \rangle + h'$. After substituting these decompositions into the original stochastic equations with some mathematical manipulation, one obtains equations for mean head and head perturbation. The mean equation cannot be solved directly because it contains some cross-covariance functions between head and medium properties such as $C_{Yh}(\mathbf{x}, \mathbf{y}) = \langle Y'(\mathbf{x})h'(\mathbf{y}) \rangle$. The equation for $\langle Y'h' \rangle$ in turn will involve some third-order terms. One can write either an implicit equation for the head perturbation or equivalently express it explicitly as integrals whose integrands contain Green's functions and other higher-order cross-covariance terms [35]. The head covariance equation is then formulated from the equation for head perturbation. Either way, these exact formulations cannot be solved without some closure approximations.

Alternatively, one can expand the hydraulic head as an infinite series in terms of the standard deviation of the medium property. More specifically, for saturated flow as considered in this study, head is expanded as an infinite series $h = \sum_{n=0}^{\infty} h^{(n)}$ in terms of σ_Y, the standard deviation of the log hydraulic conductivity. Substituting the decomposition into the original equations yields a series of recursive equations in which the equation for $h^{(n)}$ involves lower-order terms $h^{(i)}$, $i = 1, 2, \ldots, n-1$. In most existing models, the mean head is approximated up to second order in σ_Y, and the head (co)variance is approximated to first order in σ_Y^2, i.e., $C_h(\mathbf{x}, \mathbf{y}) = \langle h^{(1)}(\mathbf{x})h^{(1)}(\mathbf{y}) \rangle$. In computing the head covariance to first order in σ_Y^2, one needs to solve deterministic equations that are similar to the original equation about $2N$ times (N being the number of grid nodes): N times for solving C_{Yh} and about N times for C_h. Including higher-order terms is possible, but it will increase computational efforts drastically. Though in many cases this approach works quite well for relatively large variations in the medium properties [30, 39, 35, 18, 24], it is in general restricted to small variabilities of medium properties.

The application of Karhunen–Loève (KL) decomposition for solving stochastic boundary value problems has been pioneered by Ghanem and his coauthors [29, 11, 12, 13, 14, 15]. The essence of this technique includes discretizing the independent random process (e.g., log hydraulic conductivity) using the KL expansion and rep-

resenting the dependent stochastic process (hydraulic head or concentration) using the polynomial chaos basis. The deterministic coefficients of the dependent process in the polynomial chaos expansion are then calculated via a weighted residual procedure. Roy and Grilli [27] combined the KL decomposition and the perturbation methods to solve the steady state flow equation and obtained the mean head to first order in σ_Y and the head variance to first order in σ_Y^2. Zhang and Lu [37] evaluated higher-order approximations for the means and (co)variances of head on the basis of KL decomposition. Specifically, with the combination of KL decomposition and perturbation methods, they evaluated the mean head up to fourth order in σ_Y and the head variances up to third order in σ_Y^2. They also explored the validity of this approach for different degrees of medium variability and various correlation scales through comparisons with Monte Carlo simulations.

In this study, we compare systematically the computational cost and solution accuracy of Monte Carlo simulations, the conventional moment-equation (CME) approach, and the moment-equation approach based on the KL decomposition (KLME).

2. Stochastic differential equations. We consider transient water flow in saturated media satisfying the following continuity equation and Darcy's law [2],

$$S_s \frac{\partial h(\mathbf{x},t)}{\partial t} + \nabla \cdot \mathbf{q}(\mathbf{x},t) = g(\mathbf{x},t), \tag{2.1}$$

$$\mathbf{q}(\mathbf{x},t) = -K_s(\mathbf{x})\nabla h(\mathbf{x},t), \tag{2.2}$$

subject to initial and boundary conditions

$$h(\mathbf{x},0) = H_0(\mathbf{x}), \quad \mathbf{x} \in D, \tag{2.3}$$

$$h(\mathbf{x},t) = H(\mathbf{x},t), \quad \mathbf{x} \in \Gamma_D, \tag{2.4}$$

$$\mathbf{q}(\mathbf{x},t) \cdot \mathbf{n}(\mathbf{x}) = Q(\mathbf{x},t), \quad \mathbf{x} \in \Gamma_N, \tag{2.5}$$

where $\mathbf{q}$ is the flux, $h(\mathbf{x},t)$ is hydraulic head, $H_0(\mathbf{x})$ is the initial head in the domain D, $H(\mathbf{x},t)$ is the prescribed head on Dirichlet boundary segments Γ_D, $K_s(\mathbf{x})$ is saturated hydraulic conductivity, $Q(\mathbf{x},t)$ is the prescribed flux across Neumann boundary segments Γ_N, $\mathbf{n}(\mathbf{x}) = (n_1, \ldots, n_d)^T$ is an outward unit vector normal to the boundary $\Gamma = \Gamma_D \cup \Gamma_N$, and S_s is the specific storage.

For simplicity, in this study, we assume that porosity ϕ, specific storage S_s, and all boundary and initial conditions are deterministic, while $K_s(\mathbf{x})$ is treated as a random function and thus (2.1)–(2.5) become stochastic partial differential equations, whose solutions are no longer deterministic values but probability distributions or related statistical moments.

3. Methodology

3.1. Monte Carlo simulations. Monte Carlo simulation is one of the few methods for solving stochastic partial differential equations and perhaps is the most straightforward method in practice. This widely used approach is conceptually simple and is based on the idea of approximating a stochastic process by a large number of equally probable realizations.

The principle behind the Monte Carlo method is statistical sampling, which involves three major components. The first one is to generate multiple realizations of

the stochastic process of interest, say, hydraulic conductivity, on the basis of the given statistical moments and distributions of the process. There exist a number of methods for generating such realizations (see, for example, [22] for an assessment of some of the methods). It is important to make sure that the generated realizations of the hydraulic conductivity field honor the given statistical moments such as the mean, variance, and covariance. Plots of the local sample statistics at some representative points versus the number of realizations may be used to examine the convergence of the generated random fields. In the case that measurements are available, realizations may be conditioned at these points, i.e., honoring the measured values at these points.

The second step is to solve, for each realization, the governing equations (2.1)–(2.5) by numerical methods such as finite differences and finite elements. Note that the spatial discretization (Δ) used in the numerical methods should be inversely related to the level of spatial variability, e.g., the standard deviation of log hydraulic conductivity σ_Y. Ababou et al. [1] suggested the following relationship between η/Δ (the number of cells within each integral scale η) and σ_Y: $\eta/\Delta \gg 1+\sigma_Y$. Several studies indicated that at least five cells within each integral scale should be used in order to minimize the filtering (local averaging) effect of spatial discretization [1, 31]. Since a larger number of cells may be required to resolve the more rapidly varying hydraulic conductivity field as σ_Y increases, the maximum level of spatial variability that the Monte Carlo method could handle is limited, in practice, by the available computer power and by the ability of numerical simulators to resolve high variabilities.

The third component of the Monte Carlo method is to average over the solutions of many realizations to obtain the statistical moments or distributions of the dependent variables. Once the realizations are solved, the resulting solutions of flow quantities such as hydraulic head and flux can be averaged over all realizations to obtain statistical moments or distributions of these flow quantities. To check convergence, one may plot the local hydraulic head moments at some representative locations versus the number of Monte Carlo simulations M to identify the minimum number of realizations needed to achieve convergence in the statistical moments of the hydraulic head field. The number of simulations needed could be different for different dependent variables.

The Monte Carlo approach can handle complex geometry and boundary conditions and requires fewer assumptions than does the moment equation approach. Most importantly, the Monte Carlo approach can, in principle, deal with extremely large variability in independent variables so long as the number of realizations is large. However, this requires considerable computation and a careful examination of the results.

3.2. CME approach. The moment-equation approach is one of the alternatives for solving flow in heterogeneous porous media and has received great attention in the past two decades. The basic idea of this approach is to derive, from the original stochastic equations, a set of deterministic equations that govern the first two moments (mean and covariance) of the flow quantities.

First-order moment equations for flow in randomly heterogeneous porous media have been developed, for example, by Zhang and Lu [36]. However, for completeness, in this section we briefly outline the procedure. Though the moment-equation approach is free of assumption on parameter distributions, for the sake of comparisons with the Monte Carlo method, we assume that the hydraulic conductivity

$K_s(\mathbf{x})$ follows a log normal distribution and work with the log-transformed variable $Y(\mathbf{x}) = \ln(K(\mathbf{x})) = \langle Y(\mathbf{x})\rangle + Y'(\mathbf{x})$. The mean log saturated hydraulic conductivity $\langle Y(\mathbf{x})\rangle$ represents a relatively smooth unbiased estimate of the unknown random function $Y(\mathbf{x})$. It may be estimated using standard geostatistical methods, such as kriging, which produce unbiased estimates that honor measurements and provide uncertainty measures for these estimates. Here we assume that the log saturated hydraulic conductivity field may be conditioned at some measurement points, which means that the field may be statistically inhomogeneous. The two-point covariance function $C_Y(\mathbf{x}, \mathbf{y})$ depends on the actual locations of two points $\mathbf{x}$ and $\mathbf{y}$ rather than their separation distance, and therefore the eigenvalues and eigenfunctions of $C_Y(\mathbf{x}, \mathbf{y})$, in general, have to be solved numerically.

Because the variability of dependent variable $h(\mathbf{x}, t)$ is a function of the input variability, i.e., the variability of $Y(\mathbf{x})$, one may formally write $h(\mathbf{x}, t)$ as an infinite series as $h(\mathbf{x}, t) = h^{(0)} + h^{(1)} + h^{(2)} + \cdots$. We also expand $K_s(\mathbf{x}) = \exp[Y(\mathbf{x})] = \exp[\langle Y(\mathbf{x})\rangle + Y'(\mathbf{x})] = K_G(\mathbf{x})[1 + Y' + (Y')^2/2 + \cdots]$, where $K_G(\mathbf{x})$ is the geometric mean of $Y(\mathbf{x})$. In these series, the order of each term is with respect to σ_Y, the standard deviation of $Y(\mathbf{x})$. After combining (2.1) and (2.2), substituting expansions of $h(\mathbf{x}, t)$ and $K_s(\mathbf{x})$, and collecting terms at separate order, we obtain

$$\nabla^2 h^{(0)}(\mathbf{x}, t) + \nabla\langle Y(\mathbf{x})\rangle \cdot \nabla h^{(0)}(\mathbf{x}, t) + \frac{g(\mathbf{x}, t)}{K_G(\mathbf{x})} = \frac{S_s}{K_G(\mathbf{x})}\frac{\partial h^{(0)}(\mathbf{x}, t)}{\partial t}, \tag{3.1}$$

$$h^{(0)}(\mathbf{x}, 0) = H_0(\mathbf{x}), \quad \mathbf{x} \in \Omega, \tag{3.2}$$

$$h^{(0)}(\mathbf{x}, t) = H(\mathbf{x}, t), \quad \mathbf{x} \in \Gamma_D, \tag{3.3}$$

$$n_i(\mathbf{x})\frac{\partial h^{(0)}(\mathbf{x}, t)}{\partial x_i} = -Q(\mathbf{x}, t)/K_G(\mathbf{x}), \quad \mathbf{x} \in \Gamma_N, \tag{3.4}$$

where summation over the repeated index i is implied and for $m \geq 1$

$$\begin{aligned} &\nabla^2 h^{(m)}(\mathbf{x}, t) + \nabla\langle Y(\mathbf{x})\rangle \cdot \nabla h^{(m)}(\mathbf{x}, t) \\ &\quad = \frac{S_s}{K_G(\mathbf{x})}\sum_{k=0}^{m}\frac{(-1)^k}{m!} \times [Y'(\mathbf{x})]^k \frac{\partial h^{(m-k)}(\mathbf{x}, t)}{\partial t} - \nabla Y'(\mathbf{x}) \\ &\quad \cdot \nabla h^{(m-1)}(\mathbf{x}, t) - \frac{g(\mathbf{x}, t)}{m!\, K_G(\mathbf{x})}[-Y'(\mathbf{x})]^m, \end{aligned} \tag{3.5}$$

$$h^{(m)}(\mathbf{x}, 0) = 0, \quad \mathbf{x} \in D, \tag{3.6}$$

$$h^{(m)}(\mathbf{x}, t) = 0, \quad \mathbf{x} \in \Gamma_D, \tag{3.7}$$

$$\nabla h^{(m)}(\mathbf{x}, t) \cdot \mathbf{n}(\mathbf{x}) = -\frac{Q(\mathbf{x}, t)}{m!\, K_G(\mathbf{x})}[-Y'(\mathbf{x})]^m, \quad \mathbf{x} \in \Gamma_N. \tag{3.8}$$

Equations (3.1)–(3.4) are the governing equations for the first-order (or zeroth-order) mean head. It can be shown that $\langle h^{(0)}(\mathbf{x}, t)\rangle \equiv h^{(0)}(\mathbf{x}, t)$ and $\langle h^{(1)}(\mathbf{x}, t)\rangle \equiv 0$; thus the mean head solution up to zeroth order or first order is $h^{(0)}(\mathbf{x}, t)$. The second-order correction term $h^{(2)}$ can be solved by taking the mean of (3.5)–(3.8) with $m = 2$. The second-order mean head is $h^{[2]} = h^{(0)} + h^{(2)}$. The first-order (in terms of σ_Y^2) head covariance can be derived from (3.5)–(3.8) by setting $m = 1$, multiplying the derived equation for $h^{(1)}(\mathbf{x}, t)$ by $h^{(1)}(\boldsymbol{\chi}, \tau)$ at a different space-time location, taking

the ensemble mean, and using (3.1) and (3.4),

$$\begin{aligned}
&\frac{\partial^2 C_h(\mathbf{x},t;\boldsymbol{\chi},\tau)}{\partial x_i^2}+\frac{\partial\langle Y(\mathbf{x})\rangle}{\partial x_i}\frac{\partial C_h(\mathbf{x},t;\boldsymbol{\chi},\tau)}{\partial x_i}\\
&\quad=\frac{S_s}{K_G(\mathbf{x})}\frac{\partial C_h(\mathbf{x},t;\boldsymbol{\chi},\tau)}{\partial t}-\frac{\partial h^{(0)}(\mathbf{x},t)}{\partial x_i}\frac{\partial C_{Yh}(\mathbf{x};\boldsymbol{\chi},\tau)}{\partial x_i}\\
&\qquad-C_{Yh}(\mathbf{x};\boldsymbol{\chi},\tau)\left[\frac{\partial^2 h^{(0)}(\mathbf{x},t)}{\partial x_i^2}+\frac{\partial\langle Y(\mathbf{x})\rangle}{\partial x_i}\frac{\partial h^{(0)}(\mathbf{x},t)}{\partial x_i}\right],
\end{aligned}\tag{3.9}$$

$$C_h(\mathbf{x},0;\boldsymbol{\chi},\tau)=0,\quad \mathbf{x}\in\Omega,\tag{3.10}$$

$$C_h(\mathbf{x},t;\boldsymbol{\chi},\tau)=0,\quad \mathbf{x}\in\Gamma_D,\tag{3.11}$$

$$n_i(\mathbf{x})\left[\frac{\partial C_h(\mathbf{x},t;\boldsymbol{\chi},\tau)}{\partial x_i}+C_{Yh}(\mathbf{x};\boldsymbol{\chi},\tau)\frac{\partial h^{(0)}(\mathbf{x},t)}{\partial x_i}\right]=0,\quad \mathbf{x}\in\Gamma_N,\tag{3.12}$$

where summation over the repeated index i is implied. $C_{Yh}(\mathbf{x};\boldsymbol{\chi},\tau)$ can be obtained similarly by writing (3.5)–(3.8) of $m=1$ in terms of $(\boldsymbol{\chi},\tau)$, multiplying $Y(\mathbf{x})$ to the derived equation for $h^{(1)}(\boldsymbol{\chi},\tau)$, and taking the ensemble mean.

We may also formally write the flux $\mathbf{q}(\mathbf{x},t)$ as $\mathbf{q}(\mathbf{x},t)=\mathbf{q}^{(0)}+\mathbf{q}^{(1)}+\mathbf{q}^{(2)}+\cdots$. Then the first two moments of the flux are [35, 36]

$$\mathbf{q}^{(0)}(\mathbf{x},t)=-K_G(\mathbf{x})\nabla h^{(0)}(\mathbf{x},t),\tag{3.13}$$

$$\mathbf{q}^{(2)}(\mathbf{x},t)=-K_G(\mathbf{x})\left[Y'(\mathbf{x})\nabla h^{(1)}(\mathbf{x},t)+\frac{1}{2}Y'^2(\mathbf{x})\nabla h^{(0)}(\mathbf{x},t)+\nabla h^{(2)}(\mathbf{x},t)\right],\tag{3.14}$$

$$\begin{aligned}
&C_q(\mathbf{x},t;\boldsymbol{\chi},\tau)\\
&\quad=K_G(\mathbf{x})K_G(\boldsymbol{\chi})\Big[C_Y(\mathbf{x};\boldsymbol{\chi})\nabla_{\mathbf{x}}h^{(0)}(\mathbf{x},t)\nabla_{\boldsymbol{\chi}}h^{(0)}(\boldsymbol{\chi},\tau)\\
&\qquad+\nabla_{\mathbf{x}}h^{(0)}(\mathbf{x},t)\nabla_{\boldsymbol{\chi}}^T C_{Yh}(\mathbf{x};\boldsymbol{\chi},\tau)\\
&\qquad+\nabla_{\mathbf{x}}C_{Yh}(\boldsymbol{\chi};\mathbf{x},t)\nabla_{\boldsymbol{\chi}}^T h^{(0)}(\boldsymbol{\chi},\tau)+\nabla_{\mathbf{x}}\nabla_{\boldsymbol{\chi}}^T C_h(\mathbf{x},t;\boldsymbol{\chi},\tau)\Big].
\end{aligned}\tag{3.15}$$

The mean flux is $\mathbf{q}^{(0)}(\mathbf{x},t)$ to zeroth order or first order. The second-order correction term $\langle\mathbf{q}^{(2)}(\mathbf{x},t)\rangle$ can be derived by taking the ensemble mean of (3.14). The velocity covariance can be derived through $C_{\mathbf{v}}(\mathbf{x},t;\boldsymbol{\chi},\tau)=C_{\mathbf{q}}(\mathbf{x},t;\boldsymbol{\chi},\tau)/[\phi(\mathbf{x})\phi(\boldsymbol{\chi})]$ upon assuming deterministic porosity ϕ. Here both $C_{\mathbf{q}}$ and $C_{\mathbf{v}}$ are tensors (usually asymmetric).

3.3. Moment-equation approach based on KL decomposition

3.3.1. KL decomposition of log hydraulic conductivity. Let $Y(\mathbf{x},\omega)=\ln[K_s(\mathbf{x},\omega)]$ be a random process, where $\mathbf{x}\in D$ and $\omega\in\Omega$ (a probability space). Because the covariance function $C_Y(\mathbf{x},\mathbf{y})=\langle Y'(\mathbf{x},\omega)Y'(\mathbf{y},\omega)\rangle$ is bounded, symmetric, and positive definite, it can be decomposed into [3]

$$C_Y(\mathbf{x},\mathbf{y})=\sum_{n=1}^{\infty}\lambda_n f_n(\mathbf{x})f_n(\mathbf{y}),\tag{3.16}$$

where λ_n and $f_n(\mathbf{x})$ are called eigenvalues and eigenfunctions, respectively. Here λ_n's form a nonincreasing series and $f_n(\mathbf{x})$ are orthogonal and deterministic functions that form a complete set [23]

$$\int_D f_n(\mathbf{x})f_m(\mathbf{x})d\mathbf{x}=\delta_{nm},\quad n,m\geq 1.\tag{3.17}$$

The mean-removed stochastic process $Y'(\mathbf{x},\omega)$ can be expanded in terms of $f_n(\mathbf{x})$ as

$$Y'(\mathbf{x},\omega)=\sum_{n=1}^{\infty}\xi_n(\omega)\sqrt{\lambda_n}f_n(\mathbf{x}), \tag{3.18}$$

where $\xi_n(\omega)$ are orthogonal standard Gaussian random variables, i.e., $\langle\xi_n(\omega)\rangle=0$, and $\langle\xi_n(\omega)\xi_m(\omega)\rangle=\delta_{nm}$. The expansion in (3.18) is called the KL expansion. It can be verified that the covariance of $Y'(\mathbf{x},\omega)$ defined in (3.18) is indeed C_Y. For convenience, hereafter, we suppress the symbol ω in $Y'(\mathbf{x},\omega)$ and in other dependent functions.

Eigenvalues and eigenfunctions of a covariance function $C_Y(\mathbf{x},\mathbf{y})$ can be solved from the following Fredholm equation:

$$\int_D C_Y(\mathbf{x},\mathbf{y})f(\mathbf{x})d\mathbf{x}=\lambda f(\mathbf{y}). \tag{3.19}$$

For some special types of covariance functions, such as one-dimensional stochastic processes with an exponential covariance function $C_Y(x_1,x_2)=\sigma_Y^2\exp(-|x_1-x_2|/\eta)$, where σ_Y^2 and η are the variance and the correlation length of the process, respectively, eigenvalues and eigenfunctions can be derived analytically. For cases of two- (or three-) dimensional flows in rectangular (or brick-shaped) domains with a separable exponential covariance function, such as $C_Y(\mathbf{x},\mathbf{y})=\sigma_Y^2\exp(-|x_1-y_1|/\eta_1-|x_2-y_2|/\eta_2)$ for a two-dimensional domain $D=\{(x_1,x_2):0\le x_1\le L_1,0\le x_2\le L_2\}$, (3.19) can be solved independently for x_1 and x_2 directions to obtain eigenvalues $\lambda_n^{(1)}$ and $\lambda_n^{(2)}$ and eigenfunctions $f_n^{(1)}(x_1)$ and $f_n^{(2)}(x_2)$. These eigenvalues and eigenfunctions are then combined to form eigenvalues and eigenfunctions of C_Y [27, 37].

Equation (3.18) provides a way for generating random fields. Once eigenvalues λ_n and their corresponding eigenfunctions f_n are found, a realization can be computed simply by independently sampling a certain number of values z_n from the standard Gaussian distribution $N(0,1)$ and then computing $\sum_{n=1}^{N}z_n\sqrt{\lambda_n}f_n(\mathbf{x})$, where N is the number of terms needed to generate realizations with a given accuracy. The number N depends on the ratio of the correlation length to the domain size. Truncating the infinite series in (3.18) by a finite number of terms, we in fact ignore small scale variability of log hydraulic conductivity.

Since eigenvalues $\sqrt{\lambda_n}$ and their eigenfunctions $f_n(\mathbf{x})$ always come together, in the following derivation, we define new functions $\tilde{f}_n(\mathbf{x})=\sqrt{\lambda_n}f_n(\mathbf{x})$, and the tilde over f_n is dropped for simplicity.

3.3.2. Moment equations for head. As was done for the CME approach presented in section 3.2, we expand $h(\mathbf{x},t)$ and $K_s(\mathbf{x})$ into an infinite series and derive equations governing $h^{(m)}(\mathbf{x},t)$, $m\ge1$, i.e., (3.1)–(3.8). We further assume that $h^{(m)}(\mathbf{x},t)$ can be expanded in terms of those orthogonal Gaussian random variables ξ_n, $n=1,2,\ldots$, which are used in expanding $Y'(\mathbf{x})$ [37],

$$h^{(m)}(\mathbf{x},t)=\sum_{i_1,i_2,\ldots,i_m=1}^{\infty}\left(\prod_{j=1}^{m}\xi_{i_j}\right)h^{(m)}_{i_1,i_2,\ldots,i_m}(\mathbf{x},t), \tag{3.20}$$

where $h^{(m)}_{i_1,i_2,\ldots,i_m}(\mathbf{x},t)$ are deterministic functions to be determined. Substituting decomposition of $Y'(\mathbf{x})$, i.e., (3.18), and recursively $h^{(m)}(\mathbf{x},t)$ into (3.5)–(3.8), we obtain governing equations for $h^{(m)}_{i_1,i_2,\ldots,i_m}(\mathbf{x},t)$. For example, to determine $h_n^{(1)}(\mathbf{x},t)$, one

substitutes the expansion of $Y'(\mathbf{x})$ and $h^{(1)}(\mathbf{x},t)=\sum_{n=1}^{\infty}\xi_n\,h_n^{(1)}(\mathbf{x},t)$ into equations (3.5)–(3.8) with $m=1$ and obtains

$$\begin{aligned}\sum_{n=1}^{\infty}\xi_n\Bigg[&\nabla^2 h_n^{(1)}(\mathbf{x},t)+\nabla\langle Y(\mathbf{x})\rangle\cdot\nabla h_n^{(1)}(\mathbf{x},t)\\&-\frac{S_s}{K_G(\mathbf{x})}\left(\frac{\partial h_n^{(1)}(\mathbf{x},t)}{\partial t}-f_n(\mathbf{x})\frac{\partial h^{(0)}(\mathbf{x},t)}{\partial t}\right)\\&+\nabla f_n(\mathbf{x})\cdot\nabla h^{(0)}(\mathbf{x})-\frac{g(\mathbf{x},t)}{K_G(\mathbf{x})}f_n(\mathbf{x})\Bigg]=0.\end{aligned}\tag{3.21}$$

Because of the orthogonality of set $\{\xi_n\}$, all coefficients of the infinite series on the left-hand side of (3.21) have to be zero, which can also be seen by multiplying ξ_k on (3.21) and taking the ensemble mean. This leads to equations with initial and boundary conditions for $h_n^{(1)}(\mathbf{x},t)$:

$$\begin{aligned}&\nabla^2 h_n^{(1)}(\mathbf{x},t)+\nabla\langle Y(\mathbf{x})\rangle\cdot\nabla h_n^{(1)}(\mathbf{x},t)\\&\quad=\frac{S_s}{K_G(\mathbf{x})}\left[\frac{\partial h_n^{(1)}(\mathbf{x},t)}{\partial t}-f_n(\mathbf{x})\frac{\partial h^{(0)}(\mathbf{x},t)}{\partial t}\right]\\&\qquad-\nabla f_n(\mathbf{x})\cdot\nabla h^{(0)}(\mathbf{x})+\frac{g(\mathbf{x},t)}{K_G(\mathbf{x})}f_n(\mathbf{x}),\end{aligned}\tag{3.22}$$

$$h_n^{(1)}(\mathbf{x},0)=0,\quad \mathbf{x}\in D,\tag{3.23}$$

$$h_n^{(1)}(\mathbf{x},t)=0,\quad \mathbf{x}\in\Gamma_D,\tag{3.24}$$

$$\nabla h_n^{(1)}(\mathbf{x},t)\cdot\mathbf{n}(\mathbf{x})=\frac{Q(\mathbf{x},t)}{K_G(\mathbf{x})}f_n(\mathbf{x}),\quad \mathbf{x}\in\Gamma_N.\tag{3.25}$$

Recalling the definition of $f_n(\mathbf{x})$, it is seen that all driving terms in (3.22)–(3.25) are proportional to $\sqrt{\lambda_n}$, which decreases as n increases. This ensures that the magnitude of contribution of $h_n^{(1)}(\mathbf{x},t)$ to $h^{(1)}(\mathbf{x},t)$ decreases with n in general. This also clearly indicates that $h_n^{(1)}(\mathbf{x},t)$ are proportional to σ_Y, the standard deviation of log hydraulic conductivity. Derivation of higher-order terms $h^{(m)}_{i_1,i_2,\dots,i_m}(\mathbf{x},t)$ can be found in [37].

It is important to mention here that the second-order polynomial chaos expansions of Ghanem and Spanos [11], $\{\xi_i\xi_j-\delta_{ij},i,j=1,2,\dots\}$, are orthogonal and may be used as a basis to expand $h^{(2)}(\mathbf{x},t)$. However, because $\langle\xi_i\xi_j-\delta_{ij}\rangle\equiv 0$, the expansion $h^{(2)}(\mathbf{x},t)=\sum_{i,j=1}^{\infty}(\xi_i\xi_j-\delta_{ij})h_{ij}^{(2)}(\mathbf{x},t)$ results in $\langle h^{(2)}(\mathbf{x},t)\rangle\equiv 0$. On the other hand, if we take the ensemble mean of (3.5)–(3.8) with $m=2$, we have in general $\langle h^{(2)}(\mathbf{x},t)\rangle\neq 0$ unless the medium is homogeneous, which means that the latter expansion does not satisfy (3.5)–(3.8) of $m=2$ for flow in heterogeneous media.

We solve $h^{(m)}_{i_1,i_2,\dots,i_m}(\mathbf{x},t)$ up to fifth order, i.e., $m=5$. Once we solved $h^{(0)}(\mathbf{x},t)$, $h_n^{(1)}(\mathbf{x},t)$, $h_{ij}^{(2)}(\mathbf{x},t)$, $h_{ijk}^{(3)}(\mathbf{x},t)$, $h_{ijkl}^{(4)}(\mathbf{x},t)$, and $h_{ijklm}^{(5)}(\mathbf{x},t)$, we can directly compute the mean head and the head covariance without solving equations for $C_h(\mathbf{x},t;\boldsymbol{\chi},\tau)$ and $C_{Yh}(\mathbf{x};\boldsymbol{\chi},\tau)$, both of which are required in the CME approach. Up to fifth order in σ_Y, the head is approximated by

$$h(\mathbf{x},t)\approx\sum_{i=0}^{5}h^{(i)}(\mathbf{x},t),\tag{3.26}$$

which leads to an expression for the mean head

$$\langle h(\mathbf{x},t)\rangle \approx \sum_{i=0}^{5}\langle h^{(i)}(\mathbf{x},t)\rangle = h^{(0)}(\mathbf{x},t) + \sum_{i=1}^{\infty} h_{ii}^{(2)}(\mathbf{x},t) + 3\sum_{i,j=1}^{\infty} h_{iijj}^{(4)}(\mathbf{x},t). \tag{3.27}$$

The first term on the right-hand side of (3.27) is the zeroth-order (or first-order) approximation of the mean head: $\langle h^{(0)}(\mathbf{x},t)\rangle \equiv h^{(0)}(\mathbf{x},t)$. The second term represents the second-order (or third-order) correction to the first-order mean head, and the third term is the fourth-order (or fifth-order) correction. From (3.26) and (3.27), one can write the perturbation term up to fifth order,

$$h'(\mathbf{x},t) = h(\mathbf{x},t) - \langle h(\mathbf{x},t)\rangle \approx \sum_{i=1}^{5} h^{(i)}(\mathbf{x},t) - \langle h^{(2)}(\mathbf{x},t)\rangle - \langle h^{(4)}(\mathbf{x},t)\rangle, \tag{3.28}$$

where $\langle h^{(2)}\rangle = \langle \sum_{i,j=1}^{\infty} \xi_i\xi_j h_{ij}^{(2)}\rangle = \sum_{i=1}^{\infty} h_{ii}^{(2)}$ and $\langle h^{(4)}\rangle = 3\sum_{i,j=1}^{\infty} h_{iijj}^{(4)}$.

Equation (3.28) leads to the head covariance

$$\begin{aligned}
&C_h(\mathbf{x},t;\mathbf{y},\tau)\\
&\quad= \sum_{i=1}^{\infty} h_i^{(1)}(\mathbf{x},t)h_i^{(1)}(\mathbf{y},\tau) + 2\sum_{i,j=1}^{\infty} h_{ij}^{(2)}(\mathbf{x},t)h_{ij}^{(2)}(\mathbf{y},\tau)\\
&\quad\quad + 3\sum_{i,j=1}^{\infty} h_i^{(1)}(\mathbf{x},t)h_{ijj}^{(3)}(\mathbf{y},\tau) + 3\sum_{i,j=1}^{\infty} h_i^{(1)}(\mathbf{y},\tau)h_{ijj}^{(3)}(\mathbf{x},t)\\
&\quad\quad + \sum_{i,j,k,l,m,n=1}^{\infty} \langle \xi_{ijklmn}\rangle \Big[h_i^{(1)}(\mathbf{x},t)h_{jklmn}^{(5)}(\mathbf{y},\tau) + h_{ij}^{(2)}(\mathbf{x},t)h_{klmn}^{(4)}(\mathbf{y},\tau)\\
&\qquad\qquad + h_{ijk}^{(3)}(\mathbf{x},t)h_{lmn}^{(3)}(\mathbf{y},\tau) + h_{ijkl}^{(4)}(\mathbf{x},t)h_{mn}^{(2)}(\mathbf{y},\tau)\\
&\qquad\qquad + h_{ijklm}^{(5)}(\mathbf{x},t)h_n^{(1)}(\mathbf{y},\tau)\Big]\\
&\quad\quad - \langle h^{(2)}(\mathbf{x},t)\rangle\langle h^{(4)}(\mathbf{y},\tau)\rangle - \langle h^{(4)}(\mathbf{x},t)\rangle\langle h^{(2)}(\mathbf{y},\tau)\rangle,
\end{aligned} \tag{3.29}$$

where $\xi_{ijklmn} = \xi_i\xi_j\xi_k\xi_l\xi_m\xi_n$ for convenience. Because $\{\xi_n, n = 1, 2, \dots\}$ is a set of independent Gaussian random variables, the $\langle \xi_i\, \xi_j\, \xi_k\, \xi_l\, \xi_m\, \xi_n\rangle$ term can be easily evaluated by counting the occurrence of each ξ and using relationships $\langle \xi_i^{2k+1}\rangle = 0$ and $\langle \xi_i^{2k}\rangle = (2k-1)!!$. For instance, $\langle \xi_1\, \xi_2^2\, \xi_3^3\rangle = \langle \xi_1\rangle\langle \xi_2^2\rangle\langle \xi_3^3\rangle = 0$ and $\langle \xi_1^2\, \xi_2^4\rangle = \langle \xi_1^2\rangle\langle \xi_2^4\rangle = 1!!\cdot 3!! = 3$. The head variance up to third order in σ_Y^2 (or sixth order in σ_Y) can be derived from (3.29) as

$$\begin{aligned}
\sigma_h^2(\mathbf{x},t) &= \sum_{i=1}^{\infty}[h_i^{(1)}(\mathbf{x},t)]^2 + 2\sum_{i,j=1}^{\infty}[h_{ij}^{(2)}(\mathbf{x},t)]^2 + 6\sum_{i,j=1}^{\infty} h_i^{(1)}(\mathbf{x},t)h_{ijj}^{(3)}(\mathbf{x},t)\\
&\quad + \sum_{i,j,k,l,m,n=1}^{\infty} \langle \xi_{ijklmn}\rangle \Big[2h_i^{(1)}(\mathbf{x},t)h_{jklmn}^{(5)}(\mathbf{x},t) + 2h_{ij}^{(2)}(\mathbf{x},t)h_{klmn}^{(4)}(\mathbf{x},t)\\
&\qquad\qquad + h_{ijk}^{(3)}(\mathbf{x},t)h_{lmn}^{(3)}(\mathbf{x},t)\Big]\\
&\quad - 2\langle h^{(2)}(\mathbf{x},t)\rangle\langle h^{(4)}(\mathbf{x},t)\rangle.
\end{aligned} \tag{3.30}$$

Here the first term on the right-hand side of (3.30) represents the head variance up to first order in σ_Y^2, the second and third terms are second-order (in σ_Y^2) corrections, and the remaining terms are the third-order (in σ_Y^2) corrections.

3.3.3. Flux moments. Once we have solved for the head terms, the flux moments can be derived from (2.2). Similarly, the mean flux up to fifth order can be written as

$$\langle \mathbf{q}(\mathbf{x},t)\rangle \approx \sum_{i=0}^{5}\langle \mathbf{q}^{(i)}(\mathbf{x},t)\rangle = \mathbf{q}^{(0)}(\mathbf{x},t) + \sum_{i=1}^{\infty}\mathbf{q}_{ii}^{(2)}(\mathbf{x},t) + 3\sum_{i,j=1}^{\infty}\mathbf{q}_{iijj}^{(4)}(\mathbf{x},t), \tag{3.31}$$

where $\mathbf{q}^{(n)}_{i_1,i_2,\ldots,i_n}$, analogous to $h^{(n)}_{i_1,i_2,\ldots,i_n}$, are coefficients of expansions for $\mathbf{q}^{(n)}$. The flux covariance up to third order in σ_Y^2 is given as

$$\begin{aligned}
C_{q,rs}(\mathbf{x},t;\mathbf{y},\tau) &= \langle q_r'(\mathbf{x},t)\, q_s'(\mathbf{y},\tau)\rangle \\
&= \sum_{i=1}^{\infty} q_{i,r}^{(1)}(\mathbf{x},t)\, q_{i,s}^{(1)}(\mathbf{y},\tau) + 2\sum_{i,j=1}^{\infty} q_{ij,r}^{(2)}(\mathbf{x},t)\, q_{ij,s}^{(2)}(\mathbf{y},\tau) \\
&\quad + 3\sum_{i,j=1}^{\infty} q_{i,r}^{(1)}(\mathbf{x},t) q_{ijj,s}^{(3)}(\mathbf{y},\tau) + 3\sum_{i,j=1}^{\infty} q_{i,s}^{(1)}(\mathbf{y},\tau) q_{ijj,r}^{(3)}(\mathbf{x},t) \\
&\quad + \sum_{i,j,k,l,m,n=1}^{\infty} \langle \xi_{ijklmn}\rangle \Big[q_{i,r}^{(1)}(\mathbf{x},t) q_{jklmn,s}^{(5)}(\mathbf{y},\tau) + q_{ij,r}^{(2)}(\mathbf{x},t) q_{klmn,s}^{(4)}(\mathbf{y},\tau) \\
&\qquad\qquad + q_{ijk,r}^{(3)}(\mathbf{x},t) q_{lmn,s}^{(3)}(\mathbf{y},\tau) \\
&\qquad\qquad + q_{ijkl,r}^{(4)}(\mathbf{x},t) q_{mn,s}^{(2)}(\mathbf{y},\tau) q_{ijklm,r}^{(5)}(\mathbf{x},t) q_{n,s}^{(1)}(\mathbf{y},\tau) \Big] \\
&\quad - \langle q_r^{(2)}(\mathbf{x},t)\rangle\langle q_s^{(4)}(\mathbf{y},\tau)\rangle - \langle q_r^{(4)}(\mathbf{x},t)\rangle\langle q_s^{(2)}(\mathbf{y},\tau)\rangle, \quad r,s = 1,2,\ldots,d,
\end{aligned} \tag{3.32}$$

where subscripts r and s represent the terms corresponding to the rth and sth components of the flux field. Equation (3.32) leads to the flux variance up to third order in σ_Y^2:

$$\begin{aligned}
&\sigma_{q,s}^2(\mathbf{x},t) \\
&\quad = \sum_{i=1}^{\infty}[q_{i,s}^{(1)}(\mathbf{x},t)]^2 + 2\sum_{i,j=1}^{\infty}[q_{ij,s}^{(2)}(\mathbf{x},t)]^2 + 6\sum_{i,j=1}^{\infty} q_{i,s}^{(1)}(\mathbf{x},t) q_{ijj,s}^{(3)}(\mathbf{x},t) \\
&\quad + \sum_{i,j,k,l,m,n=1}^{\infty} \langle \xi_{ijklmn}\rangle \Big[2q_{i,s}^{(1)}(\mathbf{x},t) q_{jklmn,s}^{(5)}(\mathbf{x},t) + 2q_{ij,s}^{(2)}(\mathbf{x},t) q_{klmn,s}^{(4)}(\mathbf{x},t) \\
&\qquad\qquad + q_{ijk,s}^{(3)}(\mathbf{x},t) q_{lmn,s}^{(3)}(\mathbf{x},t) \Big] \\
&\quad - 2\langle q_s^{(2)}(\mathbf{x},t)\rangle\langle q_s^{(4)}(\mathbf{x},t)\rangle, \quad s = 1,2,\ldots,d.
\end{aligned} \tag{3.33}$$

4. Accuracy of solutions. In general, there are two types of errors associated with Monte Carlo simulation results: numerical and statistical. The former depends on the numerical method and the particular solver used as well as the spatial and temporal discretizations. The larger the spatial variability, the finer the required spatial discretization will be. The statistical errors involved in Monte Carlo simulations stem from approximating the stochastic process of interest with a finite number of realizations. To reduce this type of error, one may need to conduct a large number of simulations. The actual number of required simulations depends on the spatial variability of the process. Here in the example shown in section 6, the numerical grid used in Monte Carlo simulations is sufficiently fine to reduce the effect of numerical

discretizations, and a considerably large number of realizations are used to reduce the statistical errors. The results from Monte Carlo simulations are then considered as the "true" solutions for the flow problem, and results from both the CME and KLME approaches are compared with those from Monte Carlo simulations to validate these moment-equation approaches.

On the other hand, the conventional moment equations are derived under the assumption of small perturbations or with some kinds of closure approximations, either of which may introduce error. Compared to the Monte Carlo method, the moment-equation approach has some important distinctions. For example, the coefficients of the moment equations are relatively smooth because they are ensemble quantities. Thus the moment equations can be solved on relatively coarse grids. However, it should be noted that the equation for the head covariance is related to the cross-covariance $C_{Yh}(\mathbf{x};\mathbf{y},\tau)$, which in turn involves the derivative of the covariance function $C_Y(\mathbf{x},\mathbf{y})$. Therefore, the numerical grid for the moment-equation approach should be fine enough to more accurately approximate the derivative of $C_Y(\mathbf{x};\mathbf{y})$ over the space, which implies that the ratio of the correlation length to the grid size should be at least two.

Because the KL-based approach involves the derivative of eigenfunctions over space, it suffers from a restriction on the grid resolution similar to that for the CME approach. However, the accuracy of the KL-based approach has been evident from our previous work [37]. Zhang and Lu [37] investigated the effect of spatial variability of log hydraulic conductivity on solution accuracy for four different degrees of variability, $\sigma_Y^2 = 0.25$, 1.0, 2.0, and 4.0, for saturated flow in a rectangular domain with constant heads at both the upstream and downstream boundaries and no-flow at lateral boundaries. As expected, when σ_Y^2 is small, head variances obtained from different approaches do not have significant differences. As σ_Y^2 increases, the first-order (in σ_Y^2) head variance from the CME approach is the same as the first-order solution from the KLME approach for all four cases examined, simply implying that the number of terms ($n_1 = 100$) included in $h^{(1)}$ are adequate to approximate $h^{(1)}$. Comparing this to the first-order CME approach, with the increase of σ_Y^2, the advantage of the KLME approach is obvious. At $\sigma_Y^2 = 1.0$, the estimation error of head variance (at the center of the domain where head variance reaches its maximum) introduced by the first-order CME approach (and also the first-order KLME approach) is 17.3%, while the estimation error is 3.4% for the second-order solution of the KLME approach and 1.1% for the third-order solution of the KLME approach. At $\sigma_Y^2 = 2.0$, the estimation error of head variance for the first-order solutions is 33.6%, while they are 14.4% and 6.6%, respectively, for the second- and third-order solutions of the KLME approach.

When the porous media are strongly heterogeneous ($\sigma_Y^2 = 4.0$), although higher-order corrections of the KLME approach make some improvement on estimating the head variance over the first-order solution of the CME approach, they still deviate greatly from the Monte Carlo results. It is possible for such highly heterogeneous porous media that even higher-order terms may be needed. Another choice is to incorporate measurements on hydraulic conductivity and/or head so that the spatial variability of log hydraulic conductivity can be reduced.

In summary, for weakly heterogeneous porous media, results from both the first-order CME and first-order KLME are close to those from Monte Carlo simulations. For moderately heterogeneous porous media, such as $\sigma_Y^2 = 2.0$, results from the first-order CME deviate significantly from Monte Carlo results, while higher-order approximations from the KLME approach move closer to Monte Carlo results. For

strongly heterogeneous porous media, results from the KLME approach up to third order (in terms of σ_Y^2) are still different from Monte Carlo results.

5. Computational efficiency of solution techniques. All three formulations discussed in this paper can be solved numerically by finite element or finite difference methods, both of which will end up with a set of algebraic equations with N unknowns (N being the number of nodes in the numerical grid, which could be different for different methods) in a form of $\mathbf{Ax} = \mathbf{b}$. Two different measures have been used in comparison with computational efficiency among different methods. When we compare the computational cost required for the conventional moment method and the KL-based moment method, for simplicity, the cost is in terms of the number of times to solve sets of linear algebraic equations, because both methods yield the same matrix $\mathbf{A}$. When we compare the efficiency between Monte Carlo simulations and moment approaches, the number of floating point multiplications is used as the measure, because the Monte Carlo method requires a finer numerical grid.

5.1. CME vs. the Monte Carlo method. As mentioned in the introduction, for the CME approach, to obtain the head covariance up to first order in σ_Y^2, one needs to solve both the cross-covariance $C_{Yh}(\mathbf{x}; \mathbf{y}, \tau)$ and head covariance $C_h(\mathbf{x}, t; \mathbf{y}, \tau)$. At each time, the computational cost for both is N_{CME} (N_{CME} being the number of nodes required in the CME approach which could be different from the number of nodes required in Monte Carlo simulations). Therefore, the total cost for the first-order head covariance will be $2N_{CME}$. Even if we are interested in the head uncertainty only at some particular locations, i.e., $C_h(\mathbf{x}, t; \mathbf{y}, \tau)$ for some $\mathbf{y}$, we still need to solve $C_{Yh}(\mathbf{x}; \mathbf{y}, \tau)$ for all $\mathbf{x} \in D$, whose cost is N_{CME}.

Detailed comparison of computational efficiency of the first-order CME approach and the Monte Carlo method can be given in terms of the number of multiplications involved in each method. Assume the LU decomposition algorithm is used to solve linear algebraic equations, which requires $N^3/3$ multiplications for each equation set with N unknowns. Since each correlation length should have at least five grid lines in the Monte Carlo method and two grid lines in the CME approach, it is reasonable to assume that the relationship $N_{CME} = (2/5)^d N_{MC}$ holds, where d is dimensionality of the simulation domain. For a two-dimensional problem, the number of multiplications required for first-order CME will be $M_{CME} = (2N_{CME})N_{CME}^3/3 = 2N_{CME}^4/3 = 2[(2/5)^2 N_{MC}]^4/3 = (1.3 \times 10^{-3} \times N_{MC})N_{MC}^3/3$, compared to the number needed by the Monte Carlo method, $M_{MC} = M \times N_{MC}^3/3$, where M is the number of Monte Carlo simulations required to obtain a convergent solution. In this discussion, the fact is not utilized that at each time step the matrix $\mathbf{A}$ has to be decomposed only once in the CME method. For a small- or median-size domain, say, several to tens of thousands of nodes in the grid for Monte Carlo simulations, in general the number of realizations M needed to assure convergence of Monte Carlo simulations may be at the order of thousands, which is much larger than $1.3 \times 10^{-3} \times N_{MC}$. This indicates that for such a situation the moment approach is computationally more efficient than the Monte Carlo approach. For a large-size domain, say, millions of nodes in the grid of Monte Carlo simulations, if the variability of porous media is relatively low, the number of Monte Carlo simulations M may be at the order of thousands or less, and the Monte Carlo method can be more efficient than the first-order CME approach, because M could be less than $1.3 \times 10^{-3} \times N_{MC}$. On the basis of this discussion, by assuming $M = 1000$ the approximate crossover is on the order of one million nodes for the LU decomposition algorithm. For highly heterogeneous porous media, however, a

considerable number of realizations may be needed and the Monte Carlo method may be less efficient than the first-order CME method. Note that for such a situation the accuracy of the first-order CME approach may be low.

Similarly, for three-dimensional flow problems, one has $M_{CME} = (3.36 \times 10^{-5} \times N_{MC})N_{MC}^3/3$. Therefore, even for large-scale simulations, say, millions of nodes in the grid of Monte Carlo simulations, in general the number of required realizations $M \geq 3.36 \times 10^{-5} \times N_{MC}$, which means that the CME approach may be more efficient than the Monte Carlo approach. We have to emphasize here that the CME approach may require substantial computer memory (in two or three dimensions). For example, for a case with $N_{MC} = 10^6$, $N_{CME} = (2/5)^3 \times N_{MC} = 64{,}000$, one needs to store the cross-covariance C_{Yh}, which is a full matrix of $64{,}000 \times 64{,}000$.

If instead of LU decomposition some other numerical algorithms, such as multigrid algorithms, which need only $O(N)$ operations, are used in solving sets of linear algebraic equations, our discussion above is still valid. For multigrid algorithm in two-dimensional flow problems, the number of flow point multiplications for the CME method is $M_{CME} = 2N_{CME}^2 = 2[(2/5)^2 N_{MC}]^2 = (0.0512N_{MC}) \times N_{MC}$. Again, for a small-size domain with several thousands of grid nodes ($N_{MC} \sim 1000$), the CME method could be more efficient than the Monte Carlo method. For a large domain (say $N_{MC} \sim 10^6$), the Monte Carlo method could be more efficient that the CME method, depending on the variability of porous media. For the multigrid method, the crossover is on the order of ten thousands of grid nodes if we assume $M = 1000$.

Note that in the above discussion, we compared computational efficiency of Monte Carlo method only with the first-order CME method. If we want to find higher-order corrections, which is definitely needed for highly heterogeneous porous media, the computational burden increases drastically. For instance, to obtain the head variance up to second order in σ_Y^2, one may need to solve equations for terms such as $\langle Y'(\mathbf{x})Y'(\mathbf{y})h'(\mathbf{z},t)\rangle$ with a cost of N_{CME}^2 for each t, which is computationally very demanding for a relatively large simulation domain. In this case, the CME approach is not a good choice. In terms of computational costs, there is a crossover in the number of grid nodes, less than which the CME method is more efficient than the Monte Carlo method. However, the exact crossover is highly dependent on the choice of solver and the level of variability.

5.2. KLME vs. CME. In the KL-based perturbation approach, instead of solving the covariance equations we solve for the head terms $h^{(m)}_{i_1,i_2,\ldots,i_m}$, which are given by linear algebraic equations with N unknowns. Once with the head terms, the first two moments of head and flux can be obtained with simple algebraic operations. Because the structure of the head term equations, such as (3.22)–(3.25) for $h_i^{(1)}$, is the same as that of the moment equations $C_h(\mathbf{x},t;\boldsymbol{\chi},\tau)$, i.e., (3.9), the computational efforts for solving $h^{(m)}_{i_1,i_2,\ldots,i_m}$ on a grid of N nodes is more or less the same as that for $C_h(\mathbf{x},t;\boldsymbol{\chi},\tau)$ for each reference point $(\boldsymbol{\chi},\tau)$, or $C_{Yh}(\mathbf{x};\boldsymbol{\chi},\tau)$, for all $\mathbf{x} \in D$. In addition, as discussed previously, coefficients in equations for both CME and KLME approaches are relatively smooth, and both suffer from a similar restriction on numerical grid resolution because some coefficients are related to derivatives of functions. For these reasons, we can assume that the number of grid nodes for the CME and KLME approaches can be the same. Hence, the effectiveness of the KL-based approach largely depends on the number of times required to solve these linear algebraic equations. Due to symmetry, to obtain $h^{(m)}_{i_i,i_2,\ldots i_m}$, where $i_j = \overline{1,n}$, the cost (in terms of the number of times needed to solve linear algebraic equation with N unknowns) is $S_m = n(n+1)\cdots(n+m-1)/m!$. In the example shown in the next

section the indices for $h_i^{(1)}$, $h_{ij}^{(2)}$, $h_{ijk}^{(3)}$, $h_{ijkl}^{(4)}$, and $h_{ijklm}^{(5)}$ are 100, 20, 10, 10, and 5, respectively, i.e., index i in $h_i^{(1)}$ running up to 100 and each index in $h_{ij}^{(2)}$ running up to 20, and so on. For instance, (3.22)–(3.25) need to be solved for 100 times, and similar equations for $h_{ij}^{(2)}$ need to be solved 210 times. The total number of times needed to solve similar equations to obtain $h_i^{(1)}$, $h_{ij}^{(2)}$, $h_{ijk}^{(3)}$, $h_{ijkl}^{(4)}$, and $h_{ijklm}^{(5)}$ will be $100 + 210 + 220 + 715 + 75 = 1320$, which is less than the number of times needed for solving the $C_{Yh}(\mathbf{x}, \mathbf{y})$ and $C_h(\mathbf{x}, \mathbf{y})$ covariance equations ($2N_{CME} = 3362$, in this case) in the first-order CME approach. Note that if we are interested only in the first-order results, the cost (in terms of the number of times to solve linear equation sets with N unknowns) for the KLME approach is at the order of hundreds, compared to a few thousands for the CME approach. The total cost for solving higher-order approximations in the KLME approach is still much less than that required for the first-order CME approach. More importantly, the number of times needed to solve linear algebraic equations for the KLME approach is independent of the number of grid nodes. This makes it possible to apply the KLME approach to simulate flow and transport in more realistic large-scale problems.

The computational efforts of the KL-based approach can be reduced significantly if we take advantage of the orthogonal Gaussian random variables $\{\xi_n\}$. For example, in computing second moment terms (e.g., head variance and flux variance) up to third order in σ_Y^2, terms $h_{jklmn}^{(5)}$ and $h_i^{(1)}$ always appear together as the coefficient of term $\langle \xi_i \xi_j \xi_k \xi_l \xi_m \xi_n \rangle$. As a result, if the set of indices $\{jklmn\}$ has more than one odd number of occurrences, the term $h_{jklmn}^{(5)}$ does not need to be solved because $\langle \xi_i \xi_j \xi_k \xi_l \xi_m \xi_n \rangle \equiv 0$. For instance, the term $h_{1,3,4,4,5}^{(5)}$ can be skipped because the set $\{1, 3, 4, 4, 5\}$ has three indices that have odd numbers of occurrences. The contribution of $h_{1,3,4,4,5}^{(5)}$ to head variance and flux variance must be zero because $\langle \xi_i \xi_1 \xi_3 \xi_4^2 \xi_5 \rangle \equiv 0$, no matter what the index i is.

It has been shown [37] that for a small correlation length of log hydraulic conductivity, more terms are required to approximate $Y(\mathbf{x})$ in (3.18), and thus more terms are needed in expansions of $h^{(m)}$, which increases the computational cost of this approach. However, Zhang and Lu [37] also showed that, in the case of small correlation lengths, first-order solutions are very close to Monte Carlo results and higher-order corrections may not be needed.

5.3. KLME vs. the Monte Carlo method. Compared to the Monte Carlo method, the KLME approach solves sets of linear algebraic equations with fewer unknowns (i.e., on a coarser grid) for a smaller number of times. In addition, the coefficient matrix $\mathbf{A}$ for the KLME approach is always the same for all those equations for $h_{i_i, i_2, \ldots, i_m}^{(m)}$.

Ghanem [14] compared the Monte Carlo method and his KL-based stochastic finite element method and concluded that the former is a special case of the latter. More specifically, in his formulation, if the polynomial chaos basis in the expansion of the dependent variable is replaced by delta functions, one recovers the traditional Monte Carlo averaging. Ghanem [14] also discussed qualitatively the computational efficiency of Monte Carlo simulations and his approach. While the Monte Carlo method requires us to solve sets of linear algebraic equations with N_{MC} unknowns independently for M times, their approach requires us to solve a set of linear algebraic equations with $N \times P$, where P is the number of terms in the polynomial expansion and N is the number of nodes in the numerical grid which could be smaller than N_{MC}.

We have to emphasize a few major differences between our KLME approach and that developed by Ghanem and his coauthors on computational efficiency. While the equations for coefficients in their polynomial decomposition are fully coupled (i.e., solving linear algebraic equations $N \times P$ unknowns), in our algorithm, sets of linear algebraic equations with N unknowns are solved recursively from lower order to higher order. In addition, the number of terms in the polynomial decomposition is determined in advance in their method, while in our method, more terms can be added sequentially, if needed.

6. Illustrative examples. In this section, we give an example to illustrate how the KLME approach can significantly reduce computational efforts in computing higher-order approximations of head (and flux) for flow in a hypothetical saturated porous medium, by comparing model results with those from Monte Carlo simulations and the CME.

We consider a two-dimensional domain in a saturated heterogeneous porous medium. As shown in Figure 6.1, the flow domain is a square of size $L_1 = L_2 = 10$ $[L]$ (where L is any consistent length unit), uniformly discretized into 40×40 square elements. The no-flow conditions are prescribed at two lateral boundaries. The hydraulic head is prescribed at the left and right boundaries as 10.5 $[L]$ and 10.0 $[L]$, respectively, which produces a mean background flow from the left to the right. Two wells are located at (3.0 $[L]$, 3.0 $[L]$) and (7.0 $[L]$, 7.0 $[L]$) with strengths of -1.0 $[L/T]$ and 1.0 $[L/T]$, respectively. A negative strength represents extraction of fluid out of the domain. The statistics of the log hydraulic conductivity are given as $\langle Y \rangle = 0.0$ (i.e., the geometric mean saturated hydraulic conductivity $K_G = 1.0$ $[L/T]$, where T is any consistent time unit), $\sigma_Y^2 = 1.0$, and the correlation length $\eta = 4.0$. We will compare results from different approaches along the profile AA' which passes both wells, as indicated in Figure 6.1.

For simplicity, it is assumed in the example that the log saturated hydraulic conductivity $Y(\mathbf{x}) = \ln K_s(\mathbf{x})$ is second-order stationary with a separable exponential covariance function

$$C_Y(\mathbf{x}, \mathbf{y}) = C_Y(x_1, x_2; y_1, y_2) = \sigma_Y^2 \exp\left[-\frac{|x_1 - y_1|}{\eta} - \frac{|x_2 - y_2|}{\eta}\right], \tag{6.1}$$

where η is the correlation scale. In this case, eigenvalues λ_n, $n = 1, 2, \ldots$, and their corresponding eigenfunctions f_n, $n = 1, 2, \ldots$, can be determined analytically [37].

The number of terms included in approximating $h^{(m)}_{i_1,i_2,\ldots,i_m}$ are 100, 20, 10, 10, and 5 for $m = 1, 2, 3, 4$, and 5, respectively. It should be noted that, for the purpose of comparison, we have included large numbers of terms in these approximations. The actual numbers of terms in these approximations to achieve reasonably accurate results could be much less.

For the purpose of comparison, we conducted Monte Carlo simulations. We use 5000 two-dimensional unconditional realizations generated on the grid of 41×41 nodes with the separable covariance function given in (6.1), based on (3.18) with 200 terms. The quality of these realizations is examined by comparing their sample statistics (mean, variance, and correlation length) of these realizations with the specified mean and covariance functions. The comparisons show that the generated random fields reproduce the specified mean and covariance functions very well. The steady state, saturated flow equation is solved for each realization of the log hydraulic conductivity, using finite-element heat- and mass-transfer code (FEHM) developed by Zyvoloski et al. [40]. Then, the sample statistics of the flow fields, i.e., the mean predictions

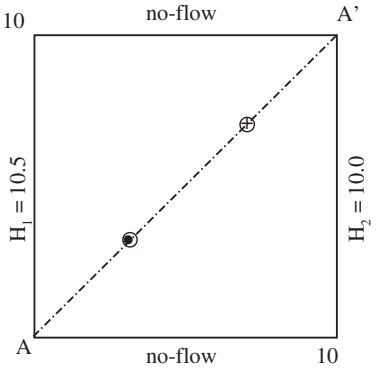

FIG. 6.1. *Boundary configuration for the illustrative example.*

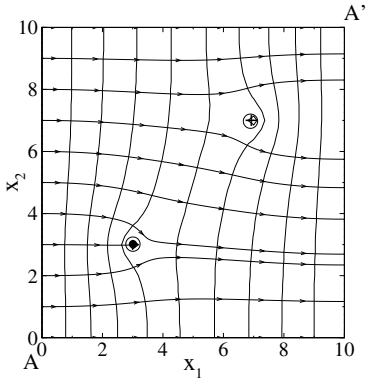

FIG. 6.2. *Mean flow field from Monte Carlo simulations.*

of head and flux as well as their associated uncertainties (variances), are computed from realizations. These statistics are considered the "true" solutions that are used to compare solution accuracy of the CME approach and the higher-order KLME approach. Figure 6.2 shows the mean flow field computed from the Monte Carlo simulations.

We also compared the results from the KLME approach against those from the first-order CME approach, i.e., the mean head and mean flux up to second order in terms of σ_Y, and head (and flux) variance up to first order in terms of σ_Y^2. The zeroth-order mean head is solved from (3.1)–(3.4), the second-order correction of mean head from the ensemble mean of (3.5)–(3.8) with $m = 2$, and the first-order head variance from solving (3.9)–(3.12). It is expected that, while the higher-order approximations of head variance and flux variance from the KLME approach should be close to Monte Carlo results, their first-order approximations shall be almost identical to those from the CME approach if n_1, the number of terms included in $h^{(1)}$, is sufficiently large. That is to say, the closeness between the first-order variances derived from the CME approach and that from the KLME approach is an indicator showing whether n_1 is large enough.

Due to the particular boundary configuration in our example, the mean head derived from different approaches does not differ significantly. To illustrate their differences more clearly, we plot the detrended mean head rather than the mean head itself. Figure 6.3(a) compares the detrended mean head obtained from Monte Carlo simulations, the zeroth-order and second-order approximations of the CME approach, and zeroth-order, second-order, and fourth-order approximations from the KLME approach along the cross section AA'. It is seen that the zeroth-order solution of mean head from the CME and KLME approaches are identical, and both deviate slightly from Monte Carlo results at or near the well locations, while the second-order approximation of mean head from both CME and KLME approaches are very close to Monte Carlo results. The contribution of fourth-order correction to mean head is very small. Figure 6.3(b) depicts the comparison of head variance derived from Monte Carlo simulations, the first-order approximations of the CME approach, and first-, second-, and third-order approximations of the KLME approach. Although the first-order approximations of the head variance from both CME and KLME approaches show a pattern similar to that of the Monte Carlo results, the discrepancies are very

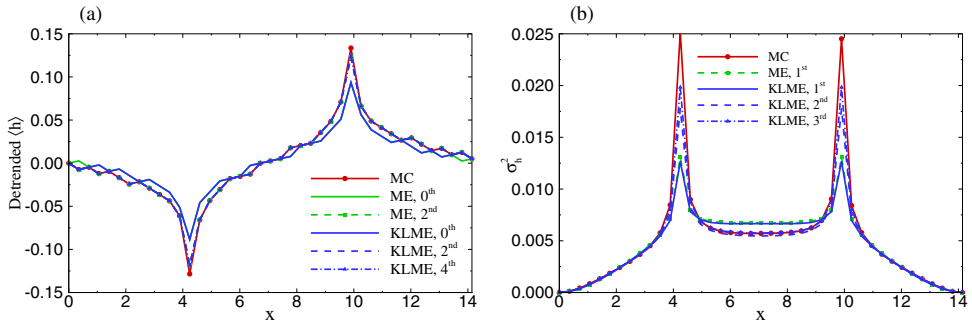

FIG. 6.3. *Comparison of* (a) *detrended mean head and* (b) *head variance derived from Monte Carlo, CME, and KLME approaches with different orders of approximations along the cross section* AA'.

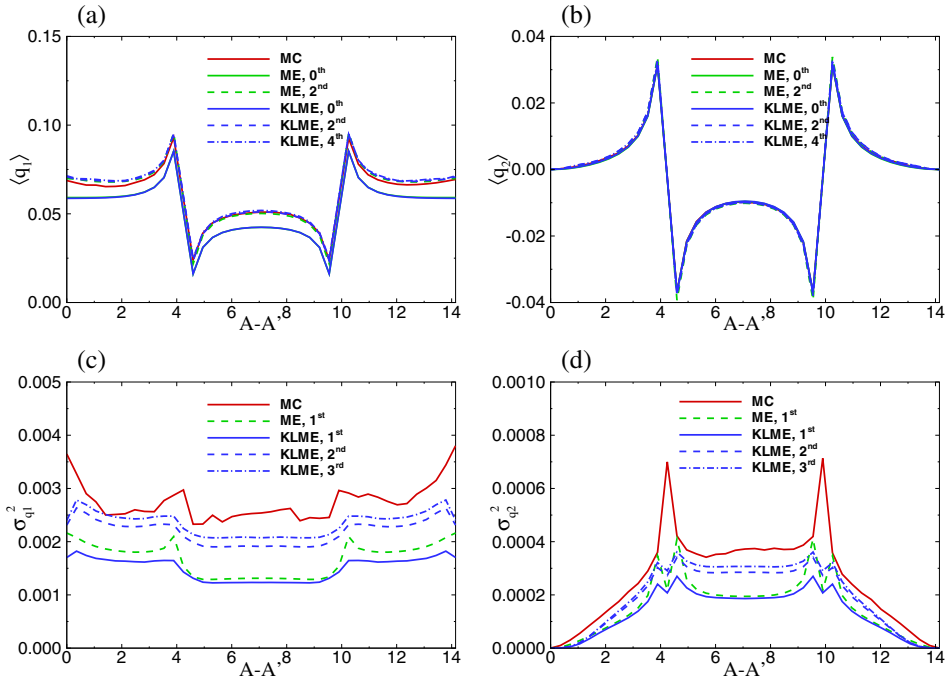

FIG. 6.4. *Comparison of* (a) *mean longitudinal flux,* (b) *mean transverse flux,* (c) *variance of longitudinal flux, and* (d) *variance of transverse derived from Monte Carlo, CME, and KLME approaches with different orders of approximations along the cross section* AA'.

large in well locations. By including second- and third-order corrections computed from the KLME approach, the results are getting close to Monte Carlo results.

Comparisons for mean flux and flux variance obtained from different approaches are illustrated in Figure 6.4. The figure shows that, for the mean flux, second-order approximations (from both CME and KLME) are accurate enough and the fourth-order contribution is very small (Figure 6.4(a)–(b)). However, flux variances computed from different approaches differ significantly for various orders of approximations.

It is seen from Figure 6.4(c)–(d) that the first-order (in terms of σ_Y^2) approximations of flux variances (both longitudinal and transverse) from the CME and the KLME approaches are very close, but they deviate significantly from the Monte Carlo results. This indicates that higher-order corrections are required to accurately approximate flux variance, and that the CME approach is not capable of fulfilling this requirement. Including the second- and third-order corrections using the KLME approach significantly improves simulation results, while the computational cost is still less than that of the CME approach up to first order.

7. Summary and conclusions. In this study, we compared solution accuracy and computational cost for the widely used Monte Carlo method and the CME approach, as well as the newly developed moment-equation approach [37] based on Karhunen–Loève decomposition, for saturated flow in randomly heterogeneous porous media. The moment-equation approach based on Karhunen–Loève decomposition (KLME) allows us to evaluate the mean head (flux) to fourth order in σ_Y and the head (flux) covariance up to third order in σ_Y^2. We demonstrated the KLME approach with an example of steady state saturated flow in a two-dimensional rectangular domain and compared our results with those from Monte Carlo simulations and from the first-order CME-based approach.

In terms of computational efficiency, the KL-based moment method is always better than both the conventional moment method and the Monte Carlo method. Regarding the computational efficiency of the Monte Carlo method and the CME approach, there is a crossover in the number of grid nodes, less than which the latter method is more efficient than the former. However, the exact crossover is highly dependent on the choice of solver and the level of variability. In general, for a small- or median-size domain, say, thousands of nodes in the grid for Monte Carlo simulations, the conventional moment approach is computationally more efficient than the Monte Carlo approach. For a large-size domain, say, millions of nodes in the grid of Monte Carlo simulations, if the variability of porous media is relatively low, the Monte Carlo method is more efficient than the first-order CME approach. However, for relatively highly heterogeneous porous media, a considerable number of realizations may be needed and the Monte Carlo method may be less efficient than the first-order CME method. For strongly heterogeneous porous media, the first-order CME method is not enough and including higher-order terms in the CME method will be infeasible because it requires one to solve sets of linear algebraic equations with N_{CME} unknowns at least N_{CME}^2 times.

The accuracy of the two moment approaches discussed in this paper depends on the degree of heterogeneity of porous media. For weakly heterogeneous porous media, the Monte Carlo method, and both the first-order CME and the KLME approaches yield similar results, which means that first-order approximations are sufficiently accurate for this case. However, the KLME approach needs only a fraction of the computation efforts required by the Monte Carlo approach and the first-order CME approach. For moderately heterogeneous porous media, such as $\sigma_Y^2 = 2$, results from the CME approach, especially the head (and flux) covariance, deviate from Monte Carlo results. In this case, higher-order corrections are needed. Including higher-order corrections using the KLME approach significantly improves simulation results. For highly heterogeneous porous media, compared to the first-order approximations, although including higher-order terms does improve the results, discrepancies still exist.

Note that if we are interested only in the first-order results, the computational costs (in terms of the number of times to solve linear algebraic equations with N

unknowns) for the KLME approach is at the order of hundreds, compared to a few thousands for the CME approach (when the number of nodes is a couple thousand). The total cost for solving higher-order approximations in the KLME approach is still much less than that required for the first-order CME approach. More importantly, the number of times to solve linear algebraic equations for the KLME approach is independent of the number of grid nodes. This makes it possible to apply the KLME approach to simulate flow and transport in more realistic large-scale problems.

REFERENCES

[1] R. D. Ababou, D. McLaughlin, L. W. Gelhar, and A. F. B. Tompson, *Numerical simulation of three-dimensional saturated flow in randomly heterogeneous porous media*, Transp. Porous Media, 4 (1989), pp. 549–565.

[2] J. Bear, *Dynamics of Fluids in Porous Media*, Dover, New York, 1972.

[3] R. Courant and D. Hilbert, *Methods of Mathematical Physics*, Interscience, New York, 1953.

[4] J. H. Cushman, *The Physics of Fluids in Hierarchical Porous Media: Angstroms to Miles*, Kluwer Academic, Norwell, MA, 1997.

[5] G. Dagan, *Stochastic modeling of groundwater flow by unconditional and conditional probabilities:* 1. *Conditional simulation and the direct problem*, Water Resour. Res., 18 (1982), pp. 813–833.

[6] G. Dagan, *A note on higher-order corrections of the head covariances in steady aquifer flow*, Water Resour. Res., 21 (1985), pp. 573–578.

[7] G. Dagan, *Flow and Transport in Porous Formations*, Springer-Verlag, New York, 1989.

[8] F. M. Deng and J. H. Cushman, *On higher-order corrections to the flow velocity covariance*, Water Resour. Res., 31 (1995), pp. 1659–1672.

[9] L. W. Gelhar, *Stochastic Subsurface Hydrology*, Prentice-Hall, Englewood Cliffs, NJ, 1993.

[10] L. W. Gelhar and C. L. Axness, *Three-dimensional stochastic analysis of macrodispersion in aquifers*, Water Resour. Res., 19 (1983), pp. 161–180.

[11] R. Ghanem and P. D. Spanos, *Stochastic Finite Elements: A Spectral Approach*, Springer-Verlag, New York, 1991.

[12] R. Ghanem and R. M. Kruger, *Numerical solution of spectral stochastic finite element systems*, Comput. Methods Appl. Mech. Engrg., 129 (1996), pp. 289–303.

[13] R. Ghanem, *Scale of fluctuation and the propagation of uncertainty in random porous media*, Water Resour. Res., 34 (1998), pp. 2123–2136.

[14] R. Ghanem, *Probabilistic characterization of transport in heterogeneous media*, Comput. Methods Appl. Mech. Engrg., 158 (1998), pp. 199–220.

[15] R. Ghanem and S. Dham, *Stochastic finite element analysis for multiphase flow in heterogeneous porous media*, Transp. Porous Media, 32 (1998), pp. 239–262.

[16] W. D. Graham and D. McLaughlin, *Stochastic analysis of nonstationary subsurface solute transport,* 1. *Unconditional moments*, Water Resour. Res., 25 (1989), pp. 215–232.

[17] A. Guadagnini and S. P. Neuman, *Nonlocal and localized analyses of conditional mean steady state flow in bounded, randomly nonuniform domains:* 1. *Theory and computational approach*, Water Resour. Res., 35 (1999), pp. 2999–3018.

[18] A. Guadagnini and S. P. Neuman, *Nonlocal and localized analyses of conditional mean steady state flow in bounded, randomly nonuniform domains:* 2. *Computational examples*, Water Resour. Res., 35 (1999), pp. 3019–3039.

[19] K. C. Hsu and S. P. Neuman, *Second-order expressions for velocity moments in two- and three-dimensional statistically anisotropic media*, Water Resour. Res., 33 (1997), pp. 625–637.

[20] K. C. Hsu, D. Zhang, and S. P. Neuman, *Higher-order effects on flow and transport in randomly heterogeneous porous media*, Water Resour. Res., 32 (1996), pp. 571–582.

[21] P. Indelman, *Averaging of unsteady flows in heterogeneous media of stationary conductivity*, J. Fluid Mech., 310 (1996), pp. 39–60.

[22] N. Liu and D. S. Oliver, *Evaluation of Monte Carlo methods for assessing uncertainty*, SPE J., June 2003.

[23] M. Loève, *Probability Theory*, 4th ed., Springer-Verlag, Berlin, 1977.

[24] Z. Lu, S. P. Neuman, A. Guadagnini, and D. M. Tartakovsky, *Conditional moment analysis of steady state unsaturated flow in bounded, randomly heterogeneous soils*, Water Resour.

Res., 38 (2002), 10.1029/2001WR000278.
[25] S. P. Neuman, *Eulerian-Lagrangian theory of transport in space-time nonstationary velocity fields: Exact nonlocal formalism by conditional moments and weak approximations*, Water Resour. Res., 29 (1993), pp. 633–645.
[26] S. P. Neuman, C. L. Winter, and C. M. Newman, *Stochastic theory of field-scale Fickian dispersion in anisotropic porous media*, Water Resour. Res., 23 (1987), pp. 453–466.
[27] R. V. Roy and S. T. Grilli, *Probabilistic analysis of the flow in random porous media by stochastic boundary elements*, Engrg. Anal. with Boundary Elements, 19 (1997), pp. 239–255.
[28] Y. Rubin, *Stochastic modeling of macrodispersion in heterogeneous media*, Water Resour. Res., 26 (1990), pp. 133–142.
[29] P. Spanos and R. Ghanem, *Stochastic finite element expansion for random media*, J. Engrg. Mech. ASCE, 115 (1989), pp. 1035–1053.
[30] D. M. Tartakovsky, S. P. Neuman, and Z. Lu, *Conditional stochastic averaging of steady state unsaturated flow by means of Kirchhoff transformation*, Water Resour. Res., 35 (1999), pp. 731–745.
[31] T. Van Lent, and P. K. Kitanidis, *Effects of first-order approximations on head and specific discharge covariances in high-contrast log conductivity*, Water Resour. Res., 32 (1996), pp. 1197–1207.
[32] C. L. Winter, C. M. Newman, and S. P. Neuman, *A perturbation expansion for diffusion in a random velocity field*, SIAM J. Appl. Math., 44 (1984), pp. 411–424.
[33] T.-C. Yeh, L. W. Gelhar, and A. L. Gutjahr, *Stochastic analysis of unsaturated flow in heterogeneous soils*: 1. *Statistically isotropic media*, Water Resour. Res., 21 (1985), pp. 447–456.
[34] D. Zhang, *Numerical solutions to statistical moment equations of groundwater flow in non-stationary, bounded heterogeneous media*, Water Resour. Res., 34 (1998), pp. 529–538.
[35] D. Zhang, *Stochastic Methods for Flow in Porous Media: Coping with Uncertainties*, Academic Press, San Diego, CA, 2002, p. 350.
[36] D. Zhang and Z. Lu, *Stochastic analysis of flow in a heterogeneous unsaturated-saturated system*, Water Resour. Res., 38 (2002), 10.1029/2001WR000515.
[37] D. Zhang and Z. Lu, *An efficient, high-order perturbation Approach for flow in random porous media via Karhunen-Loève and polynomial expansions*, J. Comput. Phys., 194 (2004), pp. 773–794.
[38] D. Zhang and S. P. Neuman, *Eulerian-Lagrangian analysis of transport conditioned on hydraulic data,* 1. *Analytical-numerical approach*, Water Resour. Res., 31 (1995) pp. 39–51.
[39] D. Zhang and C. L. Winter, *Moment equation approach to single phase flow in heterogeneous reservoirs*, Soc. Petrol. Eng. J., 4 (1999), pp. 118–127.
[40] G. A. Zyvoloski, B. A. Robinson, Z. V. Dash, and L. L. Trease, *Summary of the Models and Methods for the* FEHM *Application—A Finite-Element Heat- and Mass-Transfer Code*, Tech. report LA-13307-MS, Los Alamos National Laboratory, Los Alamos, NM, 1997.